

9. *On the Tsunami which accompanied the Niigata
Earthquake of June 16, 1964.—Source Deformation,
Propagation and Tsunami Run-up.*

By Tokutaro HATORI,

Earthquake Research Institute.

(Read Sept. 22, 1964.—Received Dec. 28, 1964.)

Abstract

The distribution of inundation height along the coast near the tsunami source shows two peaks. This feature has close relation to the deformation of the sea bottom in the source area.

From a refraction diagram, the initial crest-height at each station along the Japanese coast seems to follow Green's law. The distribution of tsunami energy seems to have been controlled by the submarine topography. The coast near the tsunami source seems to have received strong reflected waves from north Korea. As to other feature of propagation, long-waves propagated along the slope of the continental shelf seem to have existed.

From several tide-gauge records, it was concluded that tsunami waves have uniformly decayed. Decay coefficient is approximately 0.043 per hour.

1. Introduction

At 13h 02m (JST), June 16, 1964, there occurred a strong earthquake near Awashima Island in Niigata Prefecture. According to the Japan Meteorological Agency (JMA), the magnitude of the earthquake was about 7.7, and the depth 40 km, the epicenter being at 38.4°N, 139.2°E. Accompanying this earthquake, a tsunami was generated and observed on the surrounding coasts of the Japan Sea. The inundation height above M. S. L. was 4~5 m near the generating area of tsunami.

Five tsunamis have occurred in the Japan Sea since 1900 namely, the Tango earthquake of March 7, 1927,¹⁾ Oga earthquake of May 1,

1) A. IMAMURA, "On the Destructive Tango Earthquake of March 7, 1927," *Bull. Earthq. Res. Inst.*, 4 (1928), 179, (in Japanese).

1939,²⁾ Syakotan earthquake of Aug. 2, 1940³⁾, the western Aomori Prefecture earthquake of May 7, 1964, and the present one. The present tsunami is the largest in intensity of these five tsunamis and comparable with the tsunami which occurred in 1833 (Tempo 4)⁴⁾ at almost the same place.

Soon after the occurrence of the tsunami, the phenomena and damage at the coast near the generating area of the tsunami were investigated by research groups of ERI and other universities. From the results of field investigation, the distribution of inundation height and the generating area of tsunami were obtained. On the other hand, according to the Japan Hydrographic Office (JHO), the upheavals of sea bottom near the main shock have been recognized by echo-sounding after the present earthquake.

In this paper, the dislocations of sea bottom were compared with the distribution of inundation height along the coast near the tsunami source. By courtesy of JMA, Japan Geographical Survey, JHO and the Public Works Offices of several prefectures, the present writer could collect tide-gauge records of this tsunami at different stations ranging from Wakkanai to Izuhara. With the aid of these records, the problems relating to tsunami energy distribution, and edge wave propagation along the coast of Japan, reflection waves and the decay of tsunami are discussed.

2. Summary report on the tsunami observation along the coast of Japan

Almost all the tide-gauges situated near the generating area of tsunami were damaged by the earthquake. However, good records have been obtained at other tidal stations from Wakkanai to Izuhara along the coast of Japan. As the tsunami occurred in the Japan Sea, only instrumental recordings were made initially in the case of the present tsunami since actual observations were started. So the present tsunami is of the largest intensity. The features of tsunami at different localities can be seen in Table 1. The initial motion of the tsunami is *up* every-

2) F. KISHINOUE and K. IIDA, "The Tsunami that accompanied the Oga Earthquake of May 1, 1939," *Bull. Earthq. Res. Inst.*, **17** (1939), 733.

3) N. MIYABE, "Tsunami associated with the Earthquake of August 2, 1940," *Bull. Earthq. Res. Inst.*, **19** (1941), 104, (in Japanese).

4) K. MUSYA, *History of the Earthquake in Japan*, Imp. Earthq. Council, **3** (1943), 398, (in Japanese).

Table 1. Tsunami, at 13 02 June 16, 1964 (JST), as recorded by tide-gauge records.

No.	Tide station	Initial wave			Maximum wave			Δ
		Arrival time	Height*	Period	Occurred time	Height**	Period	
		d h m	cm	min	d h m	cm	min	km
1	Wakkanai	16 15 10	4		17 1 30	27	24	850
2	Osyoro	14 55	4	28	16 20 03	26	26	600
3	Esashi	13 56	4	27	20 13	59	25	390
4	Fukushima	14 00	4	23	18 20	60	22	330
5	Iwasaki	13 43	5	17	18 13	78	20	240
6	Funakawa	13 44	21	20	16 12	>240	20	150
7	Iwafune				17 00	>300	20	20
8	Matsugasaki	13 19	32	28	14 22	200	28	60
9	Kashiwazaki	13 51	11	27	15 12	24	29	140
10	Naoetsu	14 00	37	28	15 53	192	20	180
11	Toyama	13 58	19	20	15 28	52	28	280
12	Wajima	14 18	32	21	14 50	65	22	450
13	Mikuni	14 18	13	23	15 54	48	24	630
14	Tsuruga	15 00	9	23	20 53	76	20	660
15	Maizuru	15 10	4	20	23 12	82	30	700
16	Saigō	14 50	4	24	18 42	56	24	880
17	Hamada	15 20	3	22	20 10	33	12	1100
18	Izuhara				23 54	15	22	1300

* Initial crest-height above the ordinary tidal level.

** Double amplitude.

Δ Distance of propagation along a 200 m depth line.

where. In Table 1, the "initial crest-height" means the height above the ordinary tidal level and the "maximum wave-height" shows the maximal double amplitude of the sea disturbance. The symbol Δ shows the distance from the center of generating area of tsunami measured along a 200 m depth line.

The time interval between the arrival of front and the maximum waves seems to elongate with the distance of tide-gauge station as recognized, for instance, in the cases of tsunamis of 1952 (Kamchatka), 1958 and 1963 (Iturup). In the present tsunami, this relation seems to be valid as shown in Fig. 1. This phenomenon is useful for deciding when a tsunami warning may be cancelled. As a cause of this phenomenon, R. Takahasi⁵⁾ suggested the edge waves propagated along the

5) T. HATORI and R. TAKAHASI, "On the Iturup Tsunami of Oct. 13, 1963, as Observed along the Coast of Japan," *Bull. Earthq. Res. Inst.*, **42** (1964), 543.

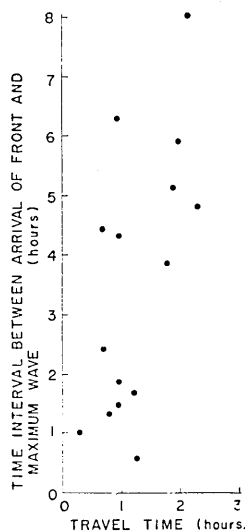


Fig. 1. The relation between travel time of the initial wave front and the time interval between arrivals of front and maximum wave.

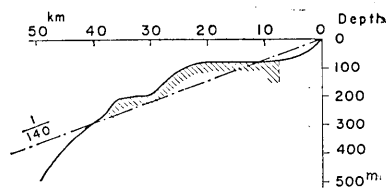


Fig. 2. The profile of the continental shelf through the center of the tsunami generating area.

continental shelf. The present tsunami, which was generated on the continental shelf along the coast of Japan, will also be the case. Fig. 2

shows the profile of the continental shelf at the center of the generating area of tsunami and the inclination of shelf is approximately $1/140$. Fig. 3 shows the relation between the distance of propagation measured along the 200 m depth line and the travel time of the maximum wave. According to Lord Kelvin, the velocity of long-wave propagated along the inclined shelf is given by the formula

$$c = \frac{Tg}{2\pi} \sin \beta$$

where T is the period of tsunami, and β is the inclination of shelf.

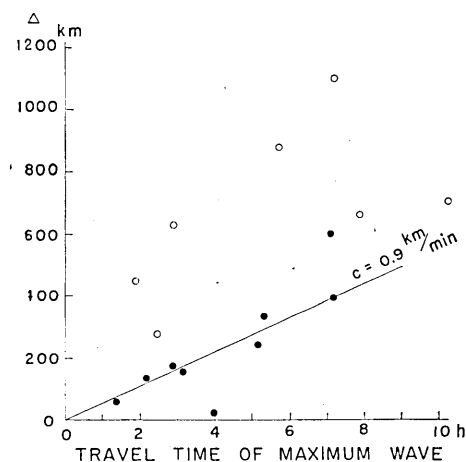


Fig. 3. The relation between the distance of propagation measured along the 200 m depth line and travel time of the maximum wave.

The period of tsunami is assumed to be 22 min in accordance with the tide gauge records. The inclination of the shelf is taken to be $\sin \beta \cong \tan \beta = 1/140$ from the profile of the shelf in Fig. 2. Result of calculation gives approximately $c=0.9$ km/min. In Fig. 3, the symbol \bullet corresponds to the localities situated to the north of Noto Peninsula. These localities are situated on a flat coast along the continental shelf.

The propagation of edge waves, therefore, seems to be possible. In the records obtained at every station, however, dispersions of waves are difficult to observe since the waves are masked with seiche oscillations of the shelf and reflection waves. Scattered circles in Fig. 3 refer to distant stations at which maximum waves seem to have arrived passing through the deep waters.

3. Sea level disturbances at the generating area of tsunami

As to the problem of directivity of tsunami, the author^{6),7)} discussed this by means of statistics and model experiments. The topographic change of the sea bottom at the tsunami source has been surveyed after various earthquakes by JHO. We could not obtain, however, information regarding the bottom disturbance owing to the long distance from the coast to the tsunami source or to the long time-interval between two surveys done before and after the earthquake. The relation between the bottom disturbance and the inundation height has hitherto been difficult to ascertain.

Fig. 4 shows the distribution of the inundation height of the present tsunami measured by the tsunami research groups of ERI⁸⁾ and Tohoku University,⁹⁾ the generating area of tsunami obtained by the inverse refraction diagram, and the upheavals of sea bottom surveyed by JHO.¹⁰⁾ The generating area of the present tsunami seems to be an ellipse which has the epicenter of the main shock (×) on its major axis. The quantity of sea bottom disturbance has enough accuracy because the sea depth was fortunately surveyed just before and after the earthquake. From the result of the survey, two zones were discovered upheaved by 6 m and 10 m.

In the following, the relation between the bottom disturbance and the distribution of inundation height is discussed in detail from the theory of tsunami generation. Fig. 5 shows the variation of relative

6) T. HATORI, "Directivity of Tsunamis," *Bull. Earthq. Res. Inst.*, **41** (1963), 61.

7) R. TAKAHASI and T. HATORI, "A Model Experiment on the Tsunami Generation from a Bottom Deformation Area of Elliptic Shape," *Bull. Earthq. Res. Inst.*, **40** (1962), 873, (in Japanese).

8) I. AIDA, K. KAJIURA, T. HATORI and T. MOMOI, "A Tsunami Accompanying the Niigata Earthquake of June 16, 1964," *Bull. Earthq. Res. Inst.*, **42** (1964), 741 (in Japanese).

9) K. NAKAMURA, "On the Field Investigation of the Niigata Tsunami," Meeting of JOTI, July 1964.

10) HYDROGRAPHIC OFFICE of JAPAN, "On the Deformation of the Sea Bottom due to the Niigata Earthquake," Monthly Meeting of ERI, July 1964.

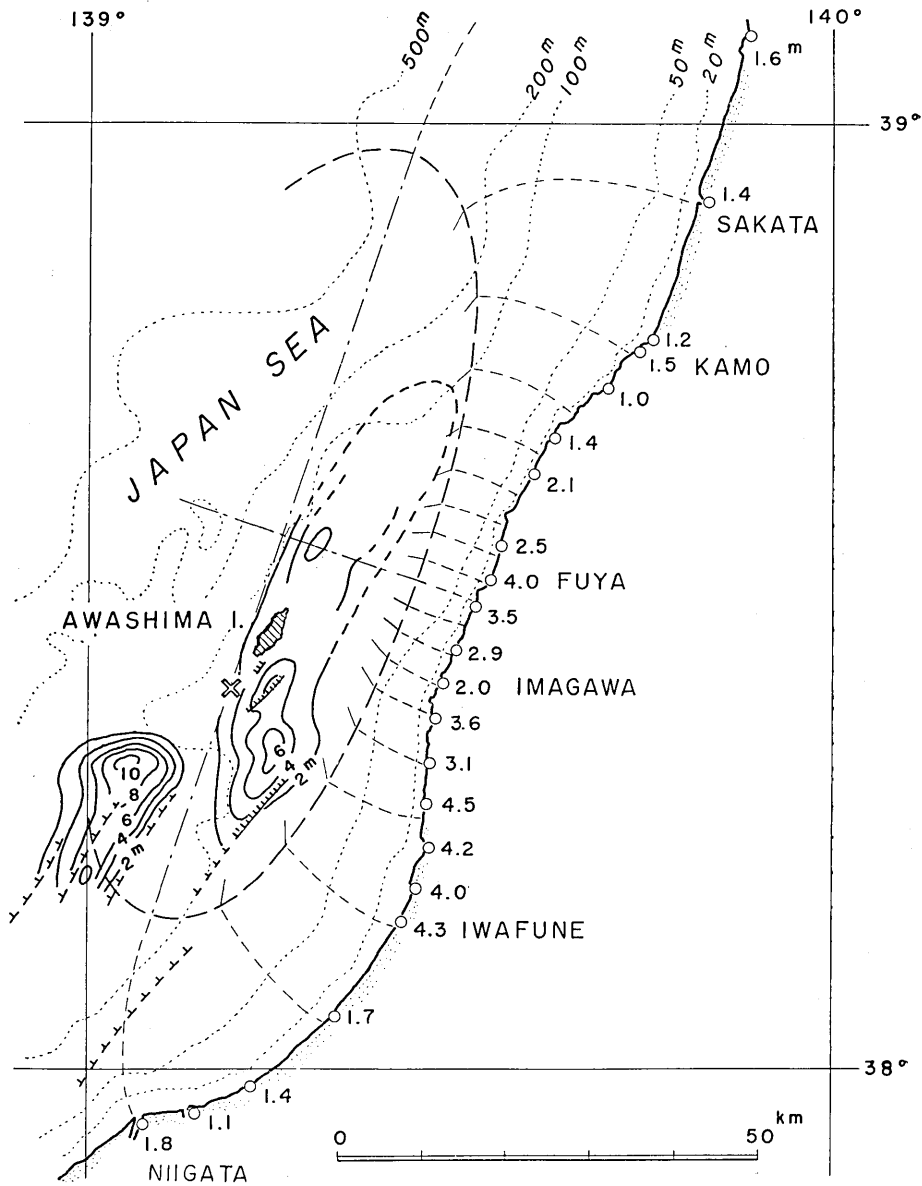


Fig. 4. The generating area of the tsunami, inundation heights above M. S. L. in meter and the bottom deformation.

inundation height with respect to the azimuth θ . Tsunami waves are assumed to originate from the elliptic margin of the generating area surrounding the sea bottom dislocations. The azimuth is measured

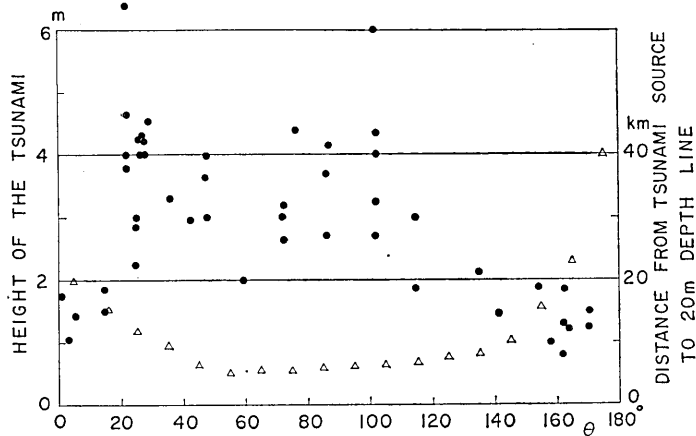


Fig. 5. Variation of relative inundation height with respect to the azimuthal direction θ .

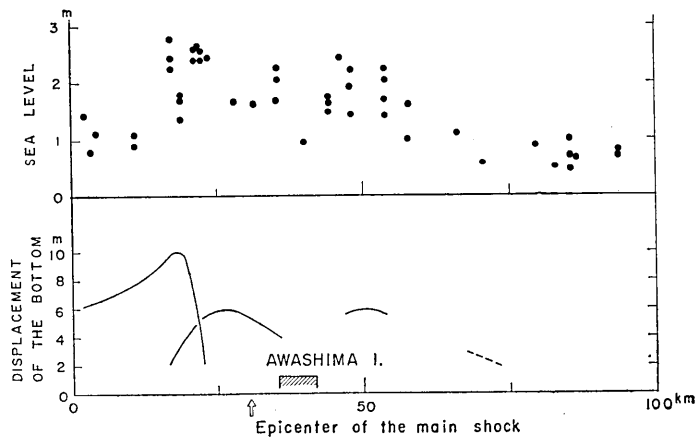


Fig. 6. Profiles of bottom deformation and the calculated sea level disturbance at the major axis of the tsunami source.

counter-clockwise from the major axis as shown in Fig 4 with the origin at the center of generating area of tsunami and is divided into multiples of ten degrees. Two peaks are found in Fig. 5. In Fig. 5 the symbol \triangle shows the distance from the margin of tsunami generating area to the 20 m depth line. The sea level disturbances at the margin of tsunami generation which correspond to the inundation heights were calculated by Green's method for each ten degrees of azimuthal angle, the coast being taken to be 5 m deep. Fig. 6 shows the profile of the sea bottom

upheavals on the major axis of the source in comparison with the calculated values of sea level disturbances. In the field investigation, the initial wave was found to be the highest along the coast near the source. The inundation heights, given in Fig. 4, are in the order of 4 m along the coast of Fuya and Iwafune, although in the neighborhood of Imagawa they were as low as 2 m. These differences of the inundation height along the coast near the tsunami source may be attributed to the feature of the upheavals of sea bottom as shown in Fig. 6.

4. Distribution of the tsunami energy

In order to know how the tsunami energy, emitted from the source, reaches different coasts of the Japan Sea, a refraction diagram was drawn as shown in Fig. 7. The tsunami source being assumed at the area

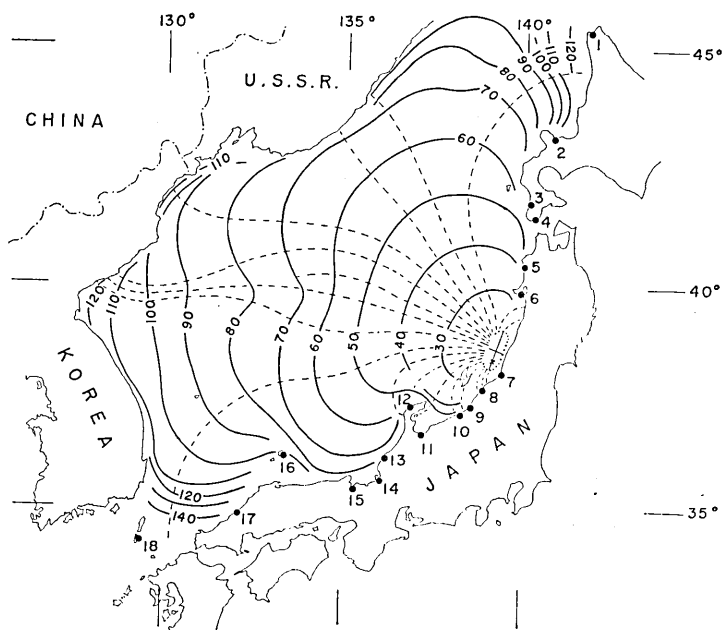


Fig. 7. Refraction diagram of wave fronts corresponding to every 10 min intervals. Numerals indicate locality shown in Table 1.

shown in Fig. 4, wave fronts have been drawn at every 10 minute intervals. As shown in Fig. 7, the travel times of the front are about 1h 30m and 2h at the coasts of USSR and North Korea respectively.

In Fig. 7, trajectories are drawn by broken curves. The azimuth

at the origin was sub-divided into five equal angles. The energy of tsunami per unit angle which is emitted from the western half at the source reached the coast with the width l between two adjacent trajectories. Fig. 8 shows the relation between the observed initial

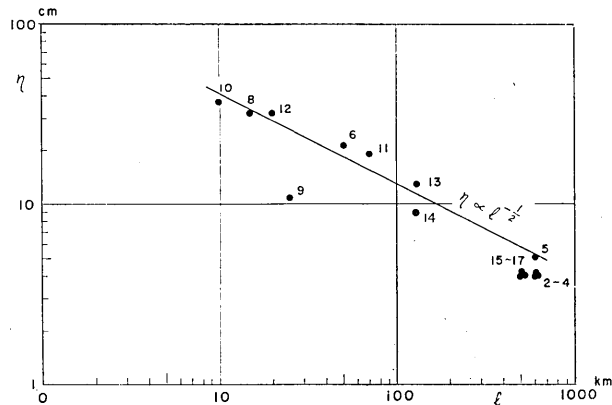


Fig. 8. The relation between the initial crest-height and the width between two adjacent trajectories at a smoothed coast line.

crest-height and the width l between two adjacent trajectories. The initial crest-height at each station along the Japanese coast seems to follow roughly Green's law $\eta \propto h^{-1/4} l^{-1/2}$, although the wave-height reduction to the value at the depth of 5 m has been neglected. The propagation of the initial wave energy from the western half of the source seems to be governed by the topography of the bottom rather than the distance from the source.

According to Nagoya University,¹¹⁾ a maximum range or double amplitude of about 2 m was observed at the north coast of Noto Peninsula. At these places tsunami energy concentrates as shown in Fig. 7. As to the tsunami along the coast of USSR and the north Korea, tsunami energy seems to be specially concentrated at the coast of north Korea as shown in Fig. 7, too.

5. Reflection waves

For the tsunamis which occur in the Japan Sea, reflection waves from USSR and Korean coasts would be observed on the coast of Japan.

11) K. IDA, "On the Field Investigation of the Niigata Tsunami," Meeting of JOTI, July 1964.

In the present case, the source of the reflection wave might be the north Korean coast as can be seen from Fig. 7. To elucidate the existence of reflection waves, the travel times of reflection waves from north Korea to Osyoro, Iwasaki, Wajima and Saigō were respectively calculated by means of inverse refraction diagrams as shown in Fig. 9.

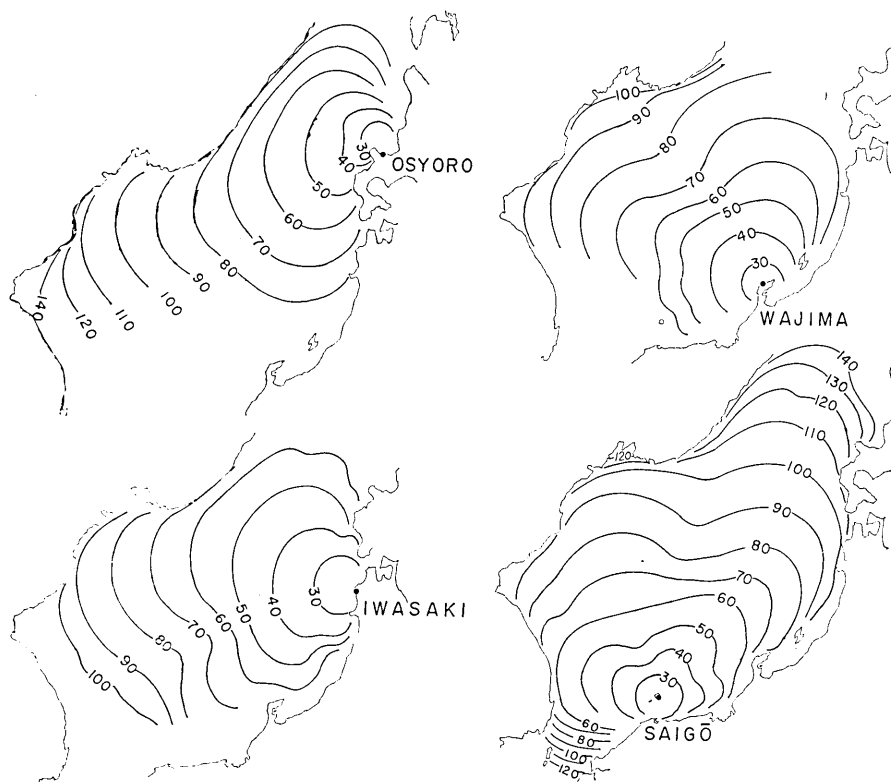


Fig. 9. Inverse refraction diagrams from Osyoro, Iwasaki, Wajima and Saigō corresponding to every 10 min intervals.

Wave fronts have been drawn every 10 min intervals. On the record of Iwafune, the maximum crest-height (initial part is locking due to the earthquake) was recorded at 3h 58m after the occurrence of the earthquake. This sharp peak seems to be reflected from the coast of north Korea as can be seen from the refraction diagram in Fig. 7. Table 2 shows the first crest-height (above ordinary tidal level) of reflection wave, travel time and the reflection angle θ , at north Korea obtained from Fig. 9.

Table 2. First crest-height of reflection wave from north Korea.

No.	Tide station	Travel time	Height	θ°
		min	cm	
1	Osyoro	248	6	130
2	Iwasaki	218	24	100
3	Iwafune	238	190*	88
4	Wajima	216	20	80
5	Saigo	211	9	70
6	Esashi	250	22	110
7	Funakawa	190	184*	95
8	Kamo	141	125*	92
9	Naoetsu	171	130*	85
10	Toyama	146	32*	82
11	Maizuru	261	34	75

* Maximum crest-height.

Fig. 10 shows the relation between the first reflected wave-height and the reflection angle, where white circles show the stations with less certainties. The reflected wave at Funakawa and Naoetsu are mixed with edge waves as shown in Fig. 3. The coast near the tsunami source seems to have received strong reflection waves from north Korea.

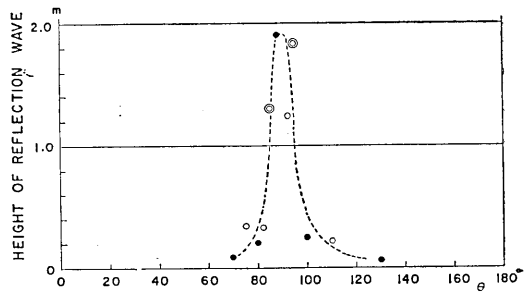


Fig. 10. Variation of the first reflected wave-height with respect to the reflected angle from north Korea.

6. Decay of tsunami waves

On the problem of decay of tsunami waves, R. Takahasi¹²⁾ indicated, in the case of the 1933 Sanriku tsunami, that the wave-heights of the sea disturbance are uniformly decayed on all Pacific coasts. This conclusion has been obtained from the investigation of features of envelopes

12) R. TAKAHASI, "Decay of Tsunami Waves," Meeting of the Seismological Society of Japan, Tokyo, April 1952.

of the wave train of tsunami records at different stations. W. H. Munk¹³⁾ obtained, in the case of the 1960 Chilean tsunami, the decay coefficients of tsunami energy in the Pacific, Atlantic and Indian Ocean to be 0.078, 0.108 and 0.174 per hour respectively. Fig. 11 shows the decay of

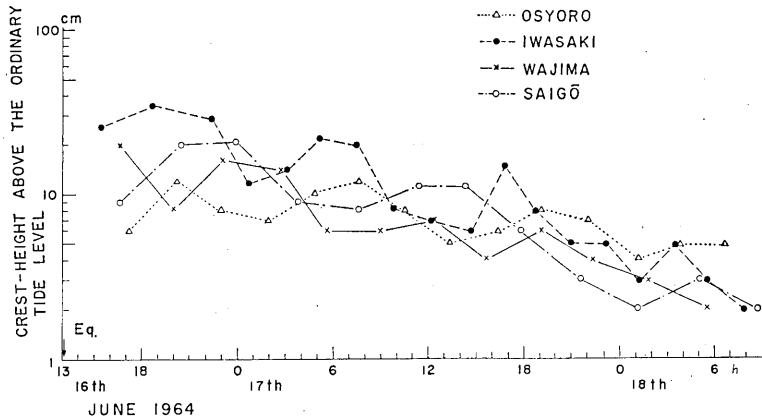


Fig. 11. Decay of tsunami waves at four stations.

tsunami waves at four stations. The periods of waves at Osyoro, Iwasaki, Wajima and Saigō are approximately 160, 180, 200 and 210 min respectively. Tsunami waves at these stations seem to have uniformly decayed according to the expression $\eta \propto e^{-\epsilon t}$. Decay coefficient ϵ obtained graphically is 0.043 per hour.

Seiches periods in the Japan Sea, according to K. Honda et al,¹⁴⁾ have been often observed to be 120~130 min and 150~180 min at many places along the Japan Sea coast. N. Kawakami¹⁵⁾ calculated these seiches as free oscillations of water in the Japan Sea as a whole. The above-mentioned periods of reflected wave are very near to the observed period of seiches of the Japan Sea. It is possible, therefore, that decay of the present tsunami waves might represent the decay of free oscillations of the Japan Sea as a whole.

7. Conclusions

From the data of field investigations, tide-gauge records and bottom

13) W. H. MUNK, "Some Comments regarding Diffusion and Absorption of Tsunamis," *Proceeding of the Tsunami meeting associated with the Tenth Pacific Science Congress* (1961), 53.

14) K. HONDA et al, "Secondary Undulations of Oceanic Tides," *J. Coll. Sci. Imp. Univ. Tokyo*, **24** (1908).

15) N. KAWAKAMI, "On the Secondary Undulations of Tides in the Japan Sea," *Umi to Sora (Sea and Sky)*, **7** (1927), 91, (in Japanese).

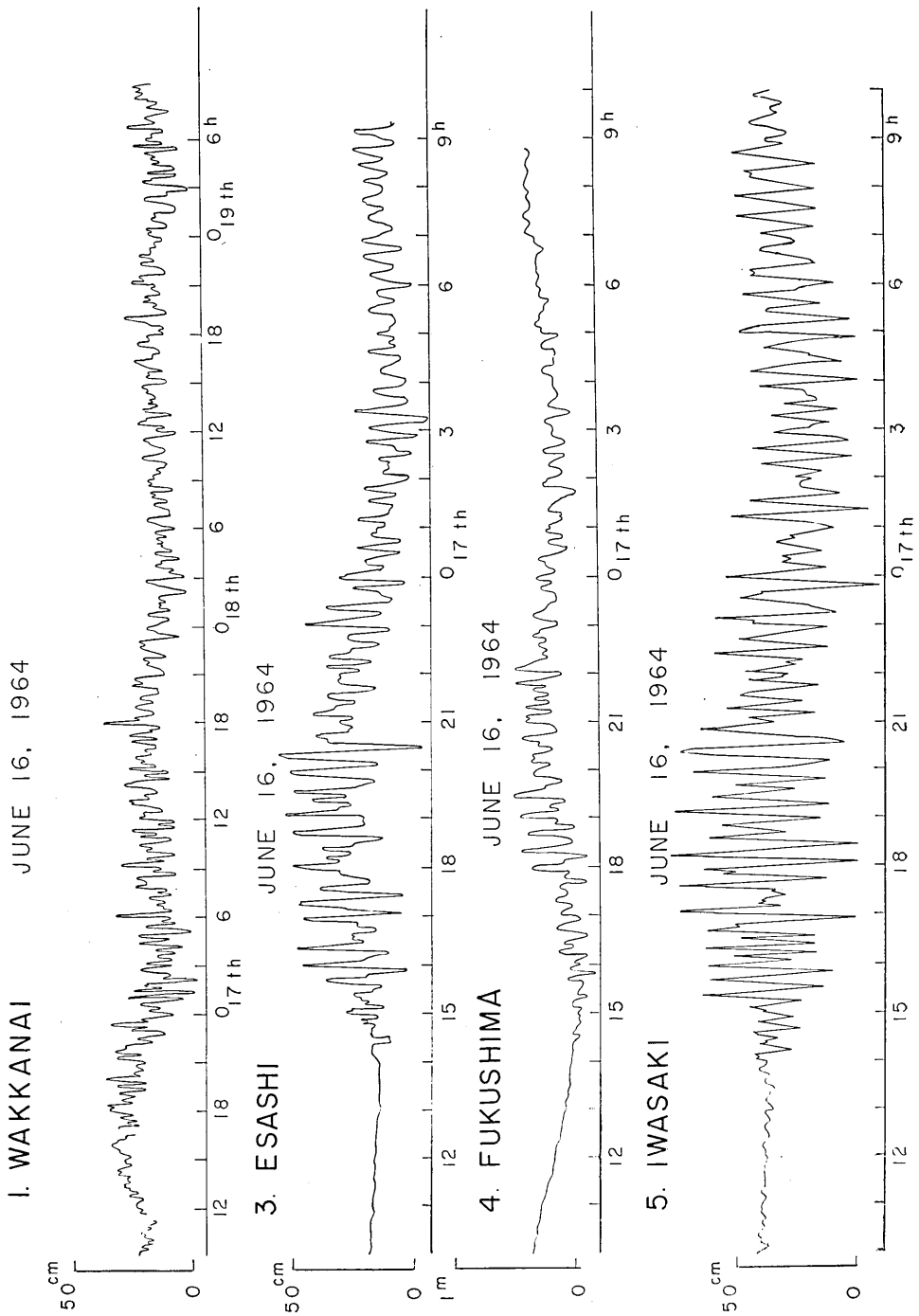


Fig. 12. Tide-gauge records at Wakkanai, Esashi, Fukushima and Iwasaki.

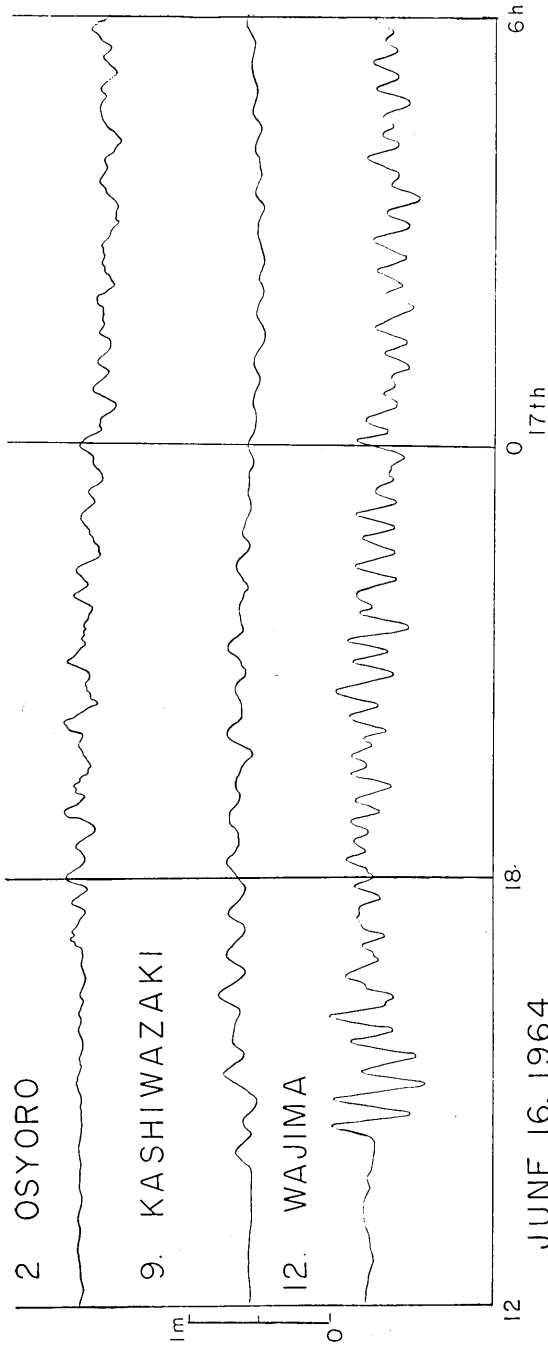


Fig. 13. Tide-gauge records at Osyoro, Kashiwazaki and Wajima.

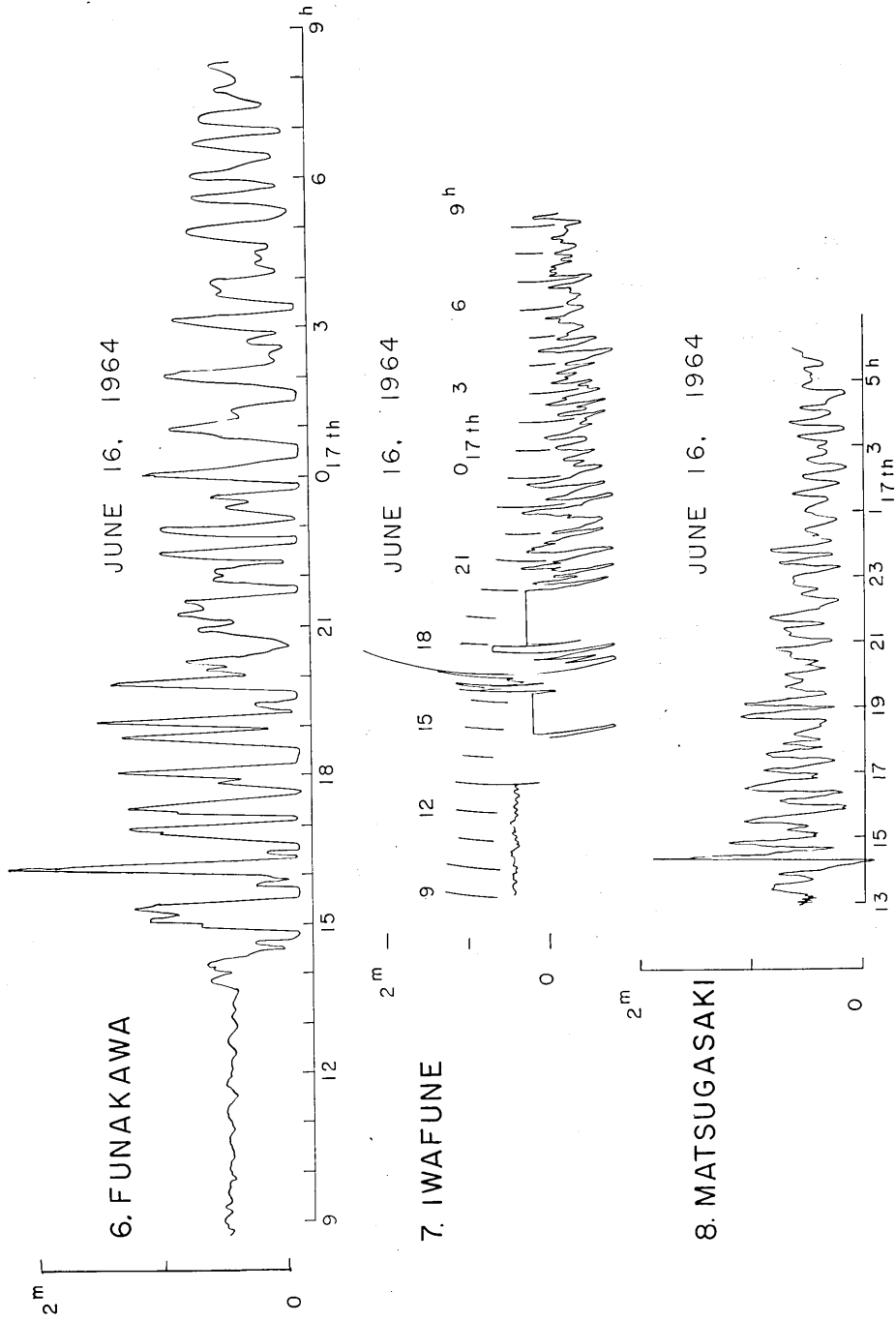


Fig. 14. Tide-gauge records at Funakawa, Iwafune and Matsugasaki.

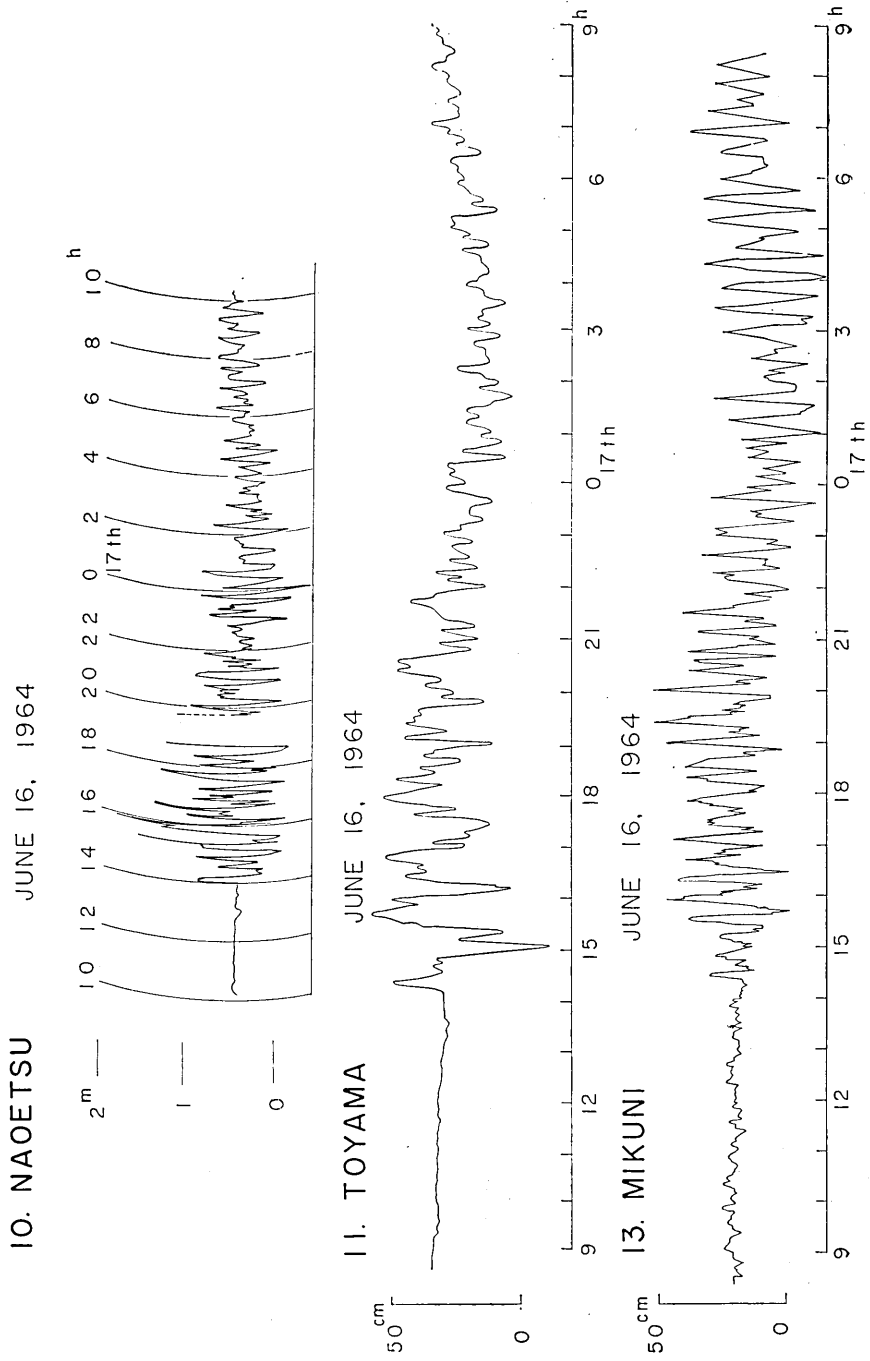


Fig. 15. Tide-gauge records at Naoetsu, Toyama and Mikuni.

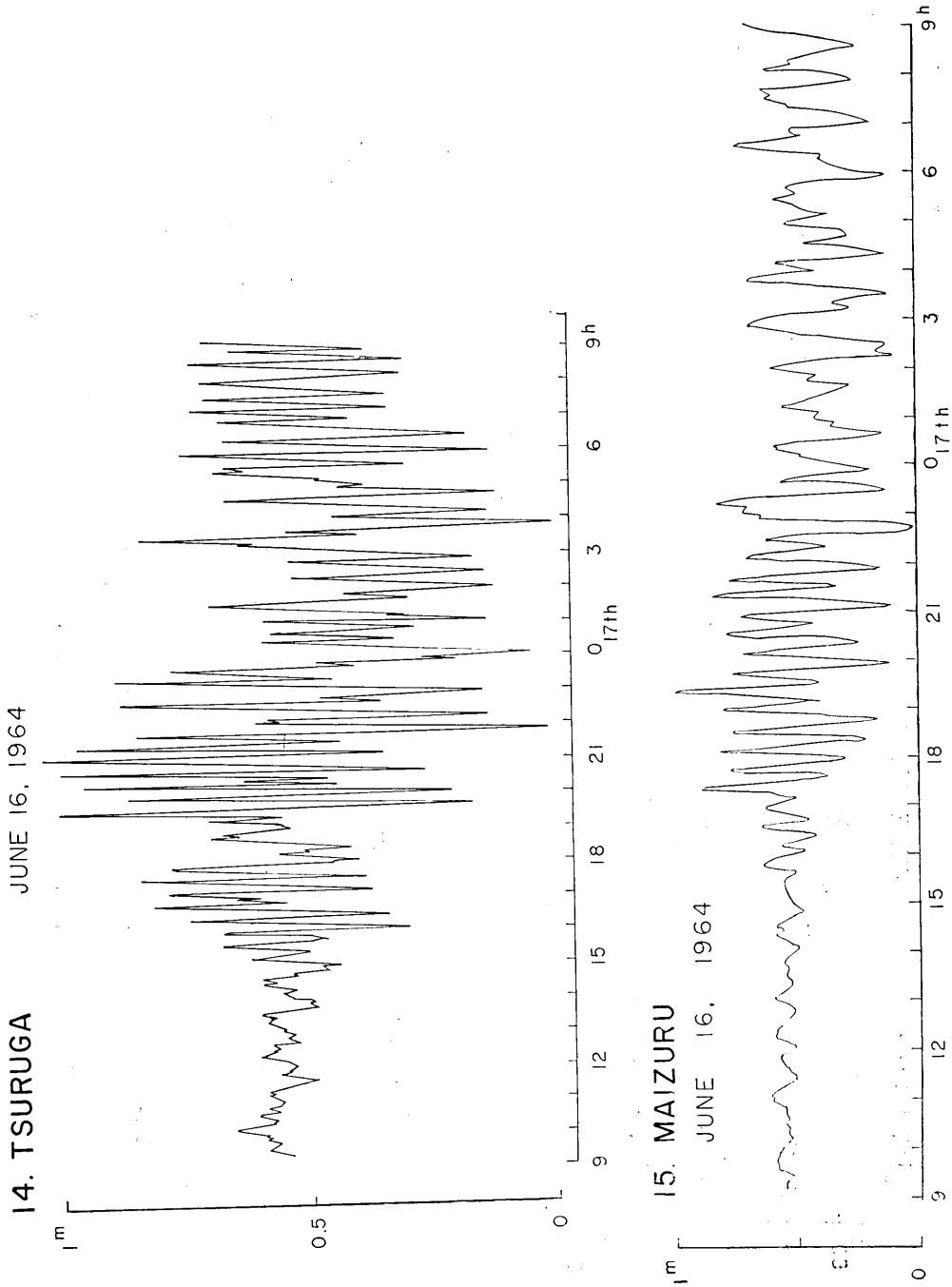


Fig. 16. Tide-gauge records at Tsuruga and Maizuru.

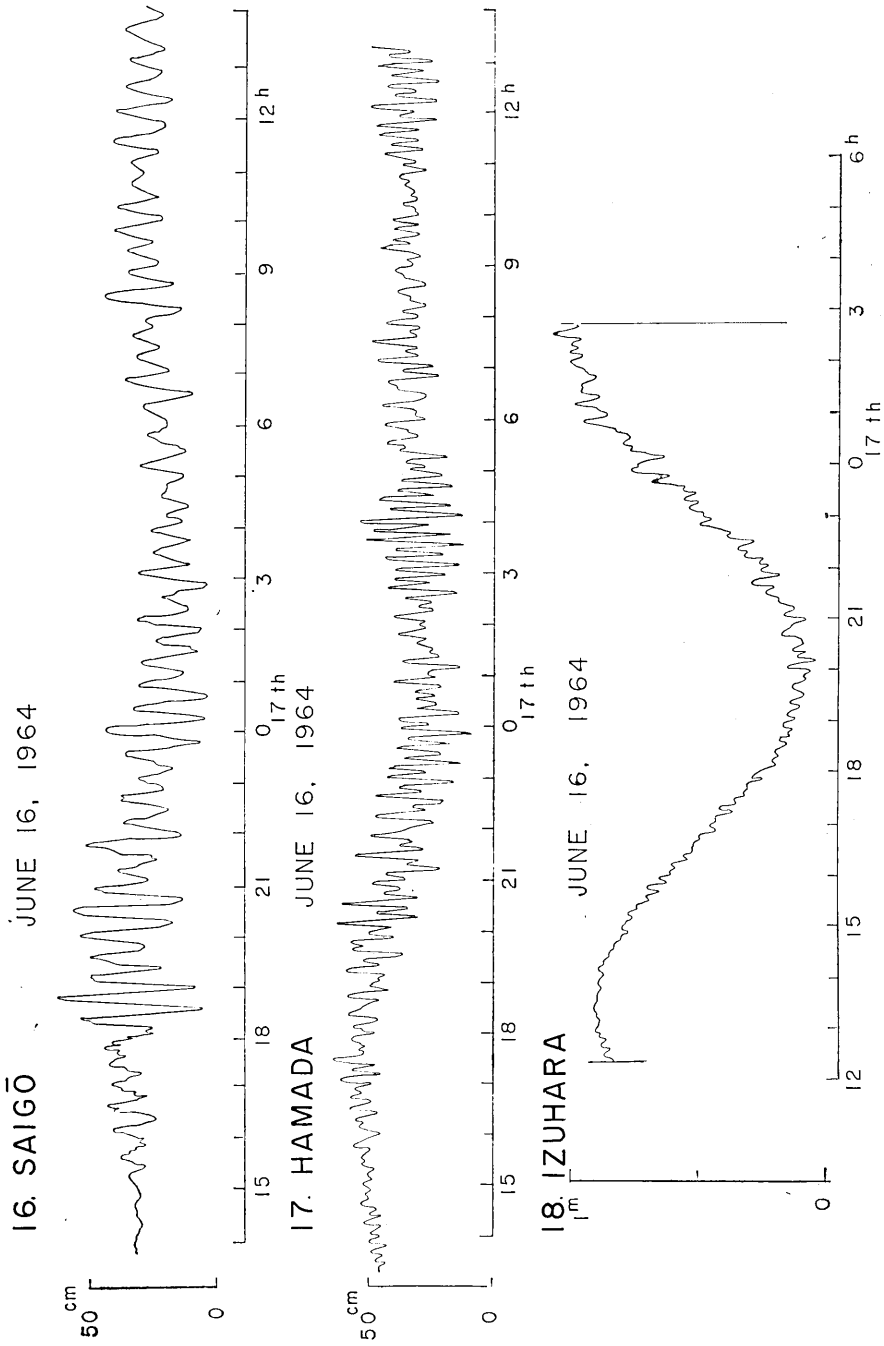


Fig. 17. Tide-gauge records at Saigō, Hamada and Izuhara.

survey, generation and propagation of the present tsunami were discussed in this paper. Characteristic oscillations of the Japan Sea as a whole, however, could not be dealt with because we have not tide-gauge records along the coasts of USSR and Korea.

In conclusion, the author wishes to express his sincere thanks to the Japan Meteorological Agency, Japan Geographical Survey Institute, Japan Hydrographic Office and the Public Works Offices of several prefectures for putting their tide-gauge records at the author's disposal. His thanks are also due to Prof. R. Takahasi for his guidance.

9. 新潟地震の津波について——浪源および伝播の問題

地震研究所 羽鳥 徳太郎

1964年6月16日13時02分、新潟県粟島附近で発生した地震(気象庁発表によれば、震央は 38.4°N , 139.2°E , 深さ40km, マグニチュード約7.7)に伴った津波は、浪源附近の沿岸で津波の高さ(M. S. L. 上)4~5mに達し、広く日本海全域で観測された。各地の概要はTable 1に示す。

この津波の規模は1900年以来、日本海に発生した4回の津波に比し最大で、1833年(天保4年)に今回とほぼ同地域で発生した津波に匹敵する。

地震直後、地震研究所その他の大学によつて、浪源周辺地域の現地調査が行われ、津波の浪源域、波高分布が明らかになつた。一方、水路部の海底測量の結果から粟島附近で、地震による顕著な海底の隆起が確認された。筆者はFig. 4に示すこれらの調査資料から、海底変動と波高分布との関係を吟味したのをはじめ、稚内~釧原間の検潮記録をもとに、津波の伝播について二、三の考察を試みた。

浪源近接地域の波高分布はFig. 5に示すように、2箇所ピークがある。この波高を沿岸の水深5mにおける値と仮定し、津波は浪源域の周辺から発射されるものと考え、Greenの定理によつて浪源域周辺の水位変動を求め、この計算値と海底変動量を浪源の長軸に透射して比較すると、Fig. 6に示したようになる。実際の調査によると、浪源附近の沿岸では第1波が最高であつたこと、浪源からほぼ同距離にある府屋、岩船において4m程度の波高があつたにもかかわらず、その中間の今川附近で2mの最低値を示したことから、浪源域での海底変動と沿岸の波高分布の間になり明瞭な対応があることを示すことが判つた。

浪源から遠い地域ほど、第1波を感じてから遅く最高波が到達することが、これまでしばしば遠地津波でみられ、高橋(1958)はこれに基づき沿岸波の存在を暗示した。今回の津波でもFig. 1に示すようにほぼこの関係がみられる。Lord Kelvinの方法で陸棚の傾斜面に伝わる速度を求めると、Fig. 3に示すように能登半島以北の比較的平坦な海岸線で観測された最高波は、陸棚のセイシュによる波高の増幅並に沿岸波を含むように思われる。

Fig. 7で浪源西半分から放射した津波エネルギーが、日本沿岸に配分された割合は、Fig. 8に示すようにほぼGreenの法則で説明でき、浪源から遠距離の地域の波高分布は伝播距離よりも寧ろ海底地形に支配されたように見える。

日本沿岸はソ連、朝鮮からの反射波を受けるが、特にFig. 7でみるごとく、津波エネルギーの集中によつて北朝鮮からの強い反射が予想される。(岩船の記録によると、浪源から放射した津波が北朝鮮で反射してきたと思われる時刻に、顕著な波高が観測された。)Fig. 9の逆伝播図を用い、各地の検潮記録で北朝鮮からの反射波の第1波を検出すると、Fig. 10に示すように、浪源附近の沿岸は北朝鮮からの強い反射を受けたようである。

Fig. 11に示す各地の津波尾部の減衰を検討すると、ほぼ一様に減衰し、波高の減衰係数は1時間につき0.043である。これは日本海における残響減衰の係数と考えられる。本多ら(1908)の調査によると、日本海の副振動の周期は120~130分および150~180分であるが、Fig. 11に示す地点での反射波の周期はこれとおおよそ一致するので、今回の津波の尾部の減衰は日本海の副振動の減衰とも考えられる。